

1 **Inhibition of Striatal-enriched Protein Tyrosine Phosphatase by**
2 **Targeting Computationally Revealed Cryptic Pockets**

3

4 Xuben Hou,^{†,§} Jin-peng Sun,[‡] Lin Ge,[‡] Xiao Liang[†], Kangshuai Li,[‡] Yingkai Zhang,^{§,⊥} and Hao
5 Fang^{†,*}

6 [†]Department of Medicinal Chemistry and Key Laboratory of Chemical Biology of Natural Products
7 (MOE), School of Pharmaceutical Science, Shandong University, Jinan, Shandong, 250012, China

8 [§]Department of Chemistry, New York University, New York, New York 10003, United States

9 [‡]Key Laboratory Experimental Teratology of the Ministry of Education and Department of Biochemistry
10 and Molecular Biology, School of Medicine, Shandong University, Jinan, Shandong 250012, China

11 [⊥]NYU-ECNU Center for Computational Chemistry, New York University–Shanghai, Shanghai
12 200122, China

13

14

Supporting Information

15

16 Corresponding author:

17 * (H.F.) Email: haofangcn@sdu.edu.cn

18

19

20

21

22

23

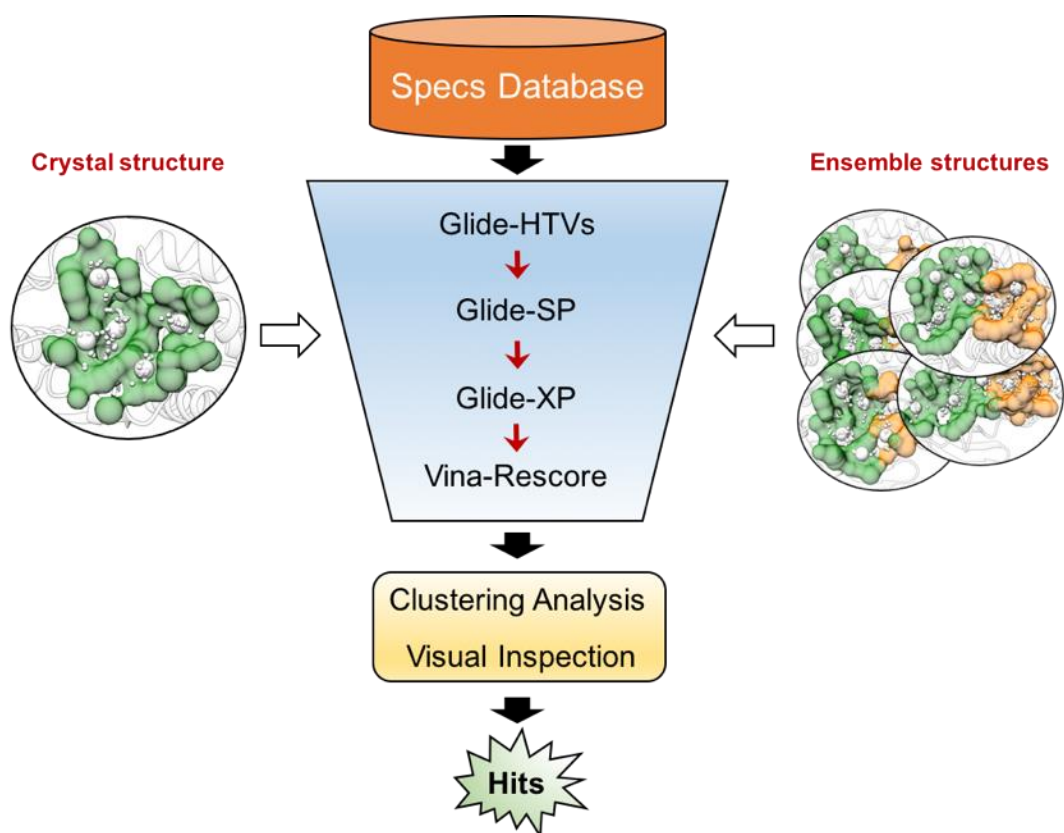
24

25

26

27

28



29

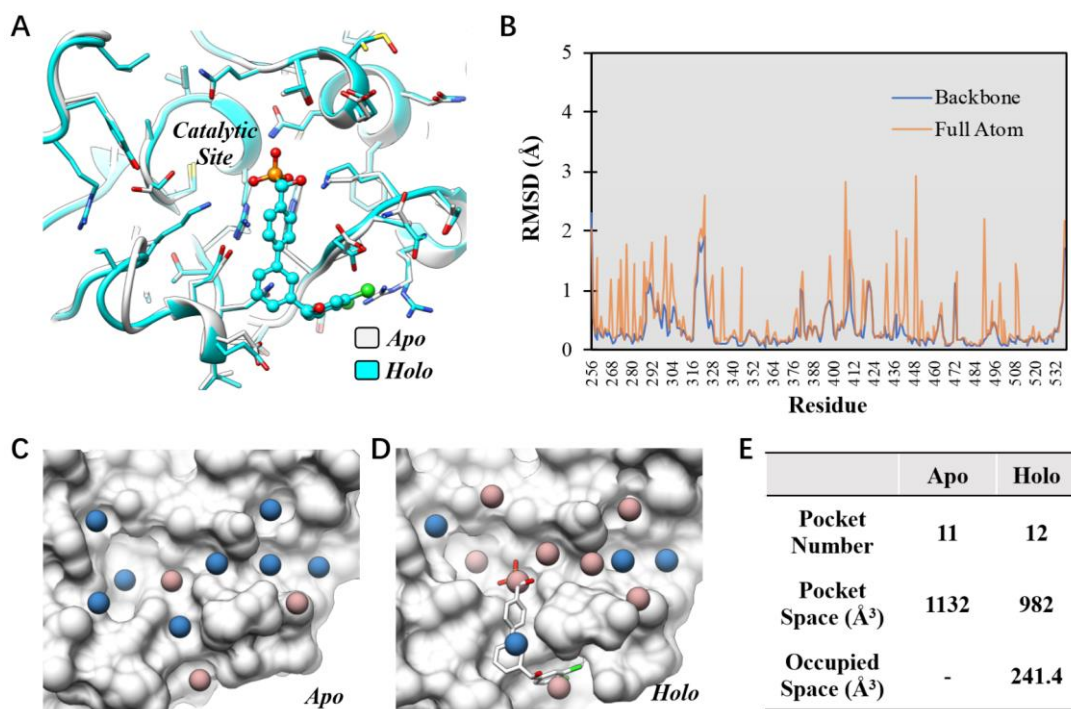
30 **Figure S1.** Structure-based virtual screening of STEP inhibitors using either crystal structure

31 (PDB: 2BV5) and ensemble structures from Markov State Model (MSM).

32

33

34



35

36 **Figure S2.** Comparison of apo (PDB: 2BV5) and holo (PDB: 5OVX) crystal structures of STEP.

37 (A) Structure alignment of apo and holo crystal structures. (B) Calculated per-residue RMSD values

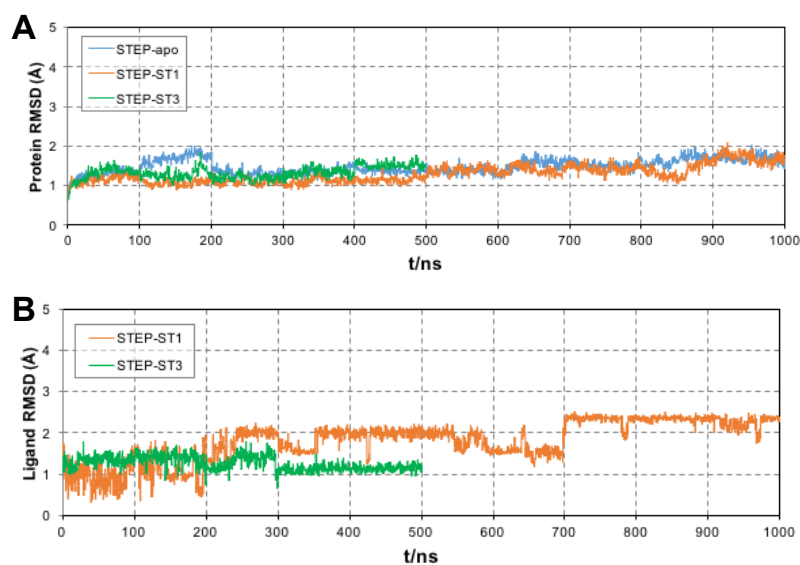
38 for backbone and full atom. (C-E) Pocket analysis of apo and holo crystal structures. All detected

39 pockets are classified as auxiliary (blue sphere) and minor pockets (rosy brown sphere) by

40 employing AlphaSpace pocket score as described before (ref). Blue spheres represent pockets with

41 score >50 and rosy brown spheres represent pockets with score <50.

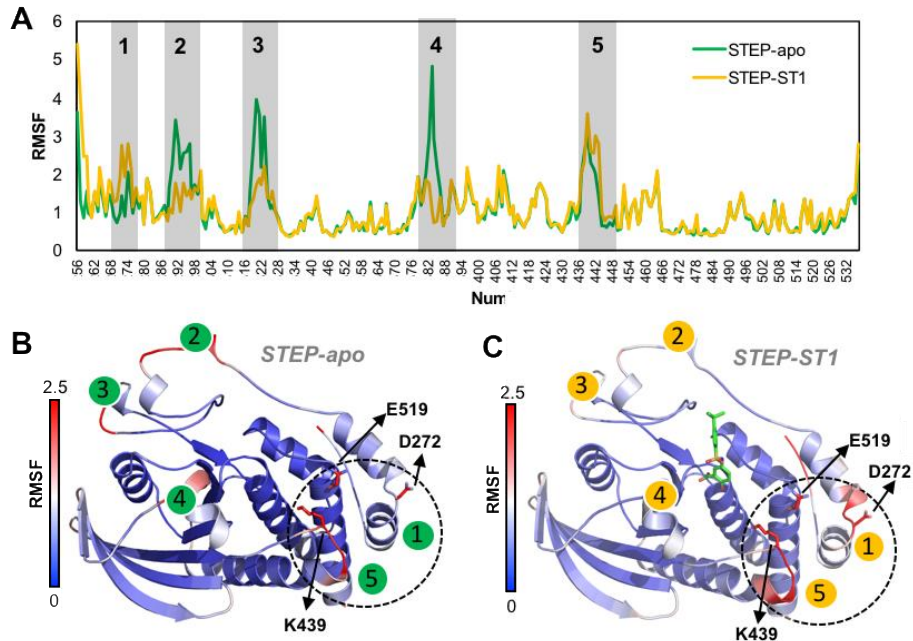
42



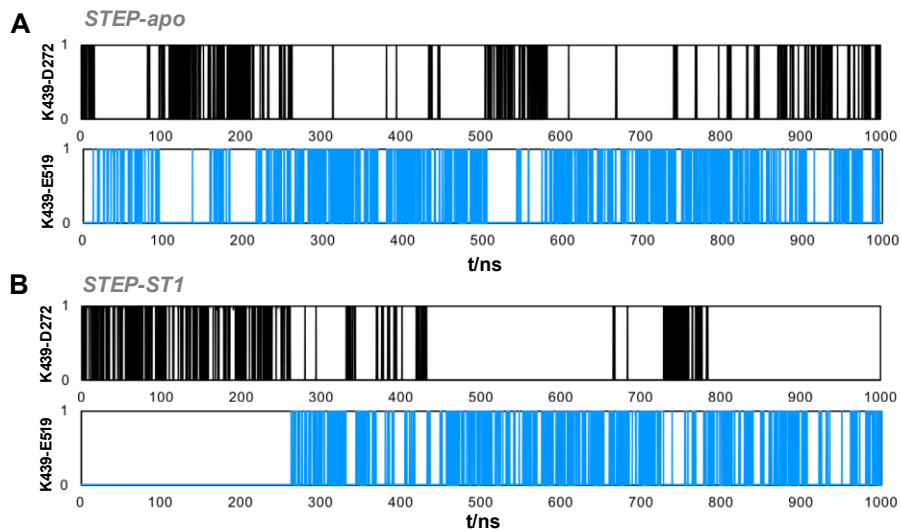
43

44 **Figure S3.** RMSD values for STEP proteins and inhibitors from MD simulations.

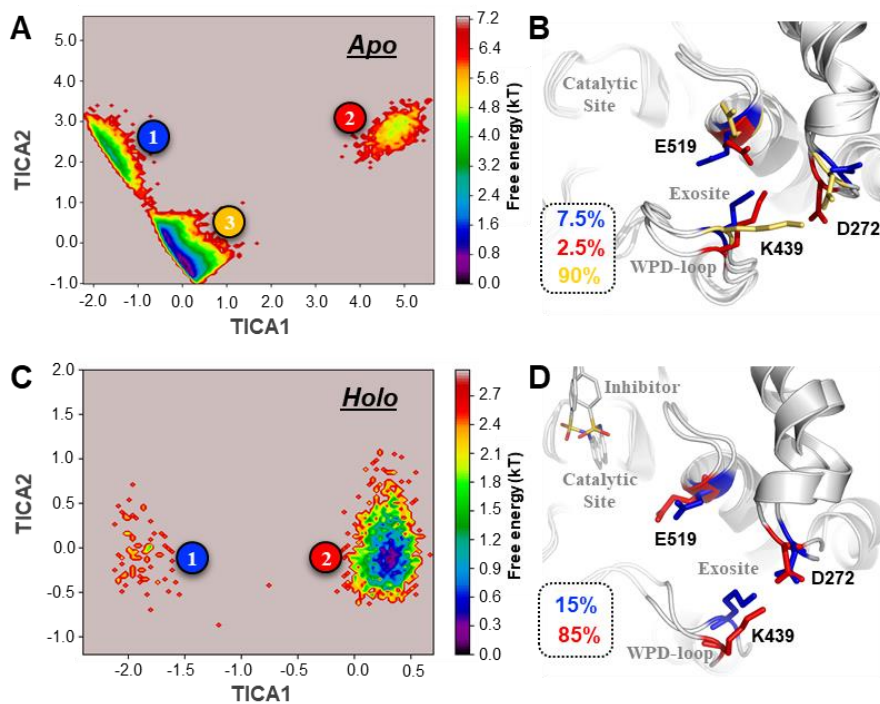
45



46
 47 **Figure S4.** Comparison of the protein flexibility of STEP with and without inhibitor binding. (A)
 48 Per-residue RMSF calculated from MD simulations of STEP-apo (green) and STEP-ST1 (yellow)
 49 systems. Conformational dynamics of STEP-apo structure (B) and STEP-ST1 complex (C) colored
 50 by their per-residue RMSF values. The crystal structure PDB:2BV5 serves as a template for
 51 comparison. The binding pose of ST1 was derived from molecular docking using the crystal
 52 structure. The color scale shows the calculated RMSF in Å.
 53



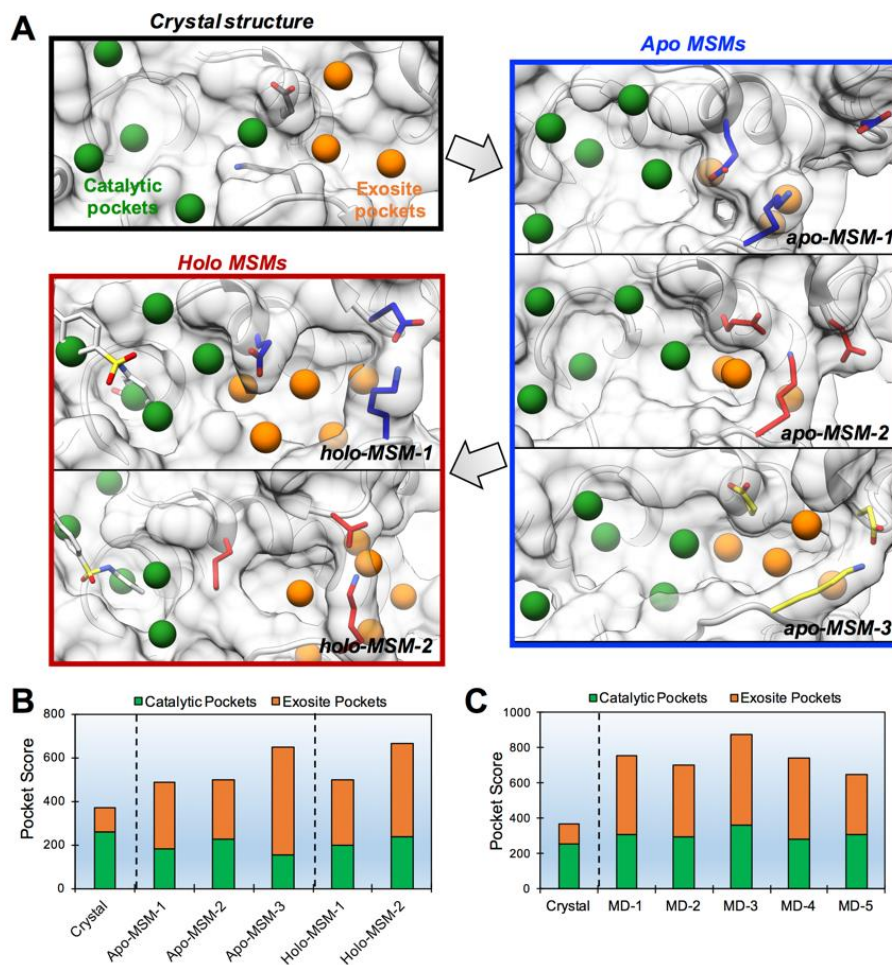
54
 55 **Figure S5.** Formation of salt-bridge interactions between K439-D272 (black) and K439-E519 (blue)
 56 during 1- μ s MD simulation on STEP-apo and STEP-ST1 systems.
 57
 58



59

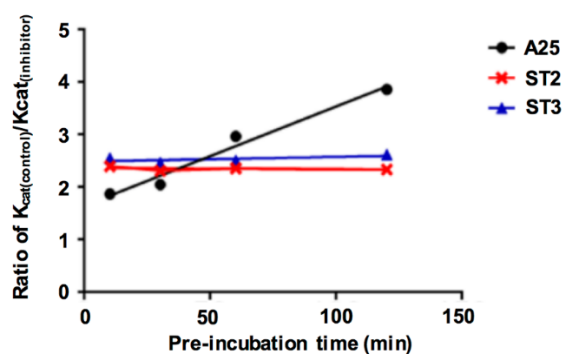
60 **Figure S6.** Free-energy landscapes of (A) the STEP-*apo* system and (C) the STEP-*ST1* system
 61 obtained via MSM analysis along the first and second TICA coordinates. Representative MD
 62 snapshots of macrostates from both (B) the STEP-*apo* system and (D) the STEP-*ST1* system. The
 63 three residues (D272, K439 and E519) used for TICA construction are shown as stick models. The
 64 location of each macrostate in the free-energy landscapes (left) is illustrated using the same color as
 65 the residues in the representative MD snapshots (right).

66



67

68 **Figure S7.** (A) Pocket analysis of apo crystal structure and representative MD snapshots from
 69 selected MSMs of STEP-apo and STEP-holo systems. Catalytic pockets and exosite pockets are
 70 presented using green and orange spheres. Key residues used for MSM construction and the
 71 inhibitor ST1 are shown as stick models. (B) Comparison of pocket scores for catalytic pocket and
 72 exosite pocket in crystal structures and selected MSMs. (C) Comparison of pocket scores of
 73 catalytic pockets and exosite pockets from crystal structure and five selected MD snapshots from
 74 MSMs.



75

76 **Figure S8.** The time-dependent ratios of $K_{cat}(\text{control})/K_{cat}(\text{inhibitor})$ for LYP inhibitor (A25) and
 77 STEP inhibitors (ST2 and ST3).

78

79

Table S1. 32 Hit compounds from apo structure-based virtual screening.

Specs ID	Structure	Specs ID	Structure
AQ-344/13518277		AQ-390/42132976	
AK-777/36504012		AR-422/41345504	
AK-968/15363155		AK-918/15000007	
AC-907/34130062		AS-871/43489763	
AE-907/30536043		AB-323/25048464	
AE-641/30108041		AH-262/34398043	
AN-465/43266004		AE-641/00770041	
AR-422/43115151		AF-399/40714286	
AI-204/43372118		AN-329/43219660	
AK-918/41371592		AG-690/15434541	
AO-476/41610193		AS-871/43476422	
AS-871/43476127		AG-205/13459129	
AE-641/00198040		AE-641/06279003	

AE-406/41056893		AI-204/31726003	
AL-281/15328110		AI-204/31682033	
AK-918/37074019		AP-906/41640126	

(ST1)

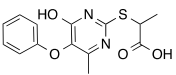
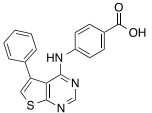
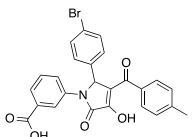
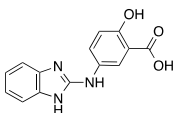
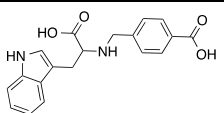
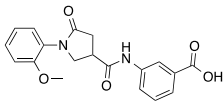
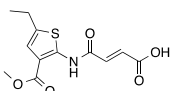
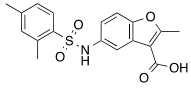
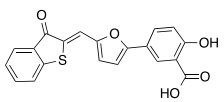
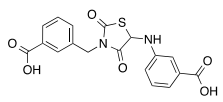
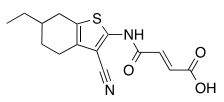
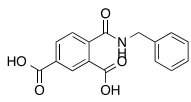
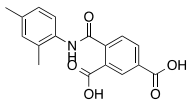
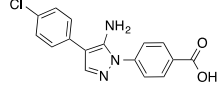
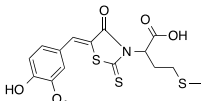
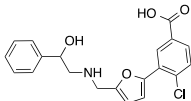
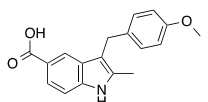
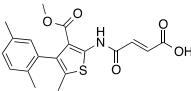
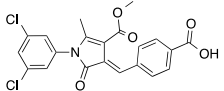
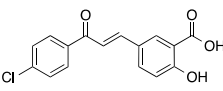
80

81

82

Table S2. 32 Hit compounds from ensemble structure-based virtual screening.

Specs ID	Structure	Specs ID	Structure
AP-853/43386858		AO-022/43452506	
	(ST8)		(ST5)
AK-968/40709324		AP-853/43445418	
AE-848/14138703		AF-399/15285005	
	(ST6)		
AQ-149/13890403		AN-989/41838787	
AO-022/40415417		AG-205/13052034	
			(ST2)
AI-204/33265041		AE-406/41057026	
			(ST10)

AG-205/34704054		AP-906/41027680	 (ST12)
AO-022/43452907		AQ-086/43457605	
AN-465/43411092		AK-918/42815229	
AK-968/15364107		AQ-390/42861800	 (ST4)
AG-205/33667015	 (ST3)	AP-893/40872493	
AK-968/12515454	 (ST11)	AP-263/12245698	
AP-263/12245694		AG-670/42920055	
AF-399/37181008		AN-465/43421754	
AQ-086/43383935	 (ST7)	AK-968/15363412	 (ST9)
AO-081/41131569		AP-185/43377268	

83

84

85 **Table S3.** Specs ID for **ST2** analogs and **ST3** analogs.

Compound	Specs ID	Compound	Specs ID
ST2-1	AG-690/13153056	ST3-1	AG-690/11835134
ST2-2	AG-690/12869899	ST3-2	AG-205/11234130
ST2-3	AG-690/13153051	ST3-3	AN-023/13438050
ST2-4	AG-690/13153079	ST3-4	AG-205/37007075
ST2-5	AG-690/37099003	ST3-5	AO-081/40681146

86

87

88

89 **Table S4.** Inhibitory activities of selected compounds against wide type STEP and F523A mutant.

Protein	Inhibitory activity (μM)			
	ST2	ST2-5	ST3	ST3-5
WT	9.7 \pm 2.6	7.7 \pm 1.5	10.7 \pm 0.9	7.5 \pm 1.2
F523A	31.3 \pm 8.5	>100	99.7 \pm 10.9	81.9 \pm 9.2

90

91

92

93 **Video Captions**94 **Video S1.** MD simulation of STEP-apo system. STEP protein is shown as white surface with
95 catalytic site and exosite site colored in green and orange yellow, respectively.

96

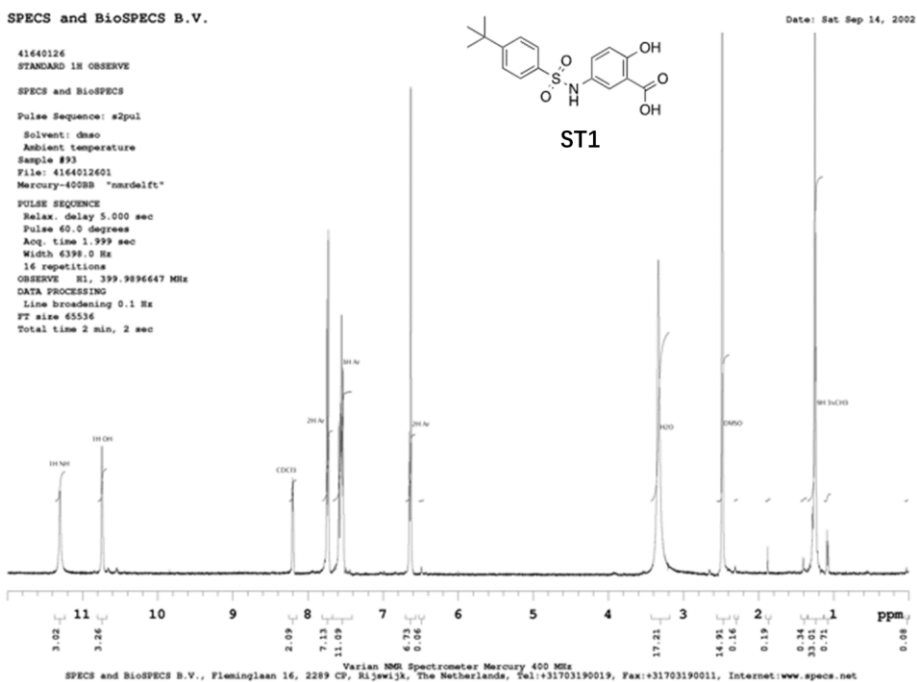
97 **Video S2.** MD simulation of STEP-**ST3** system. STEP protein is shown as white surface with
98 catalytic site and exosite site colored in green and orange yellow, respectively. Inhibitor **ST3** are
99 shown as spheres and colored according to atom type.

100

101

102 ¹H-NMR for representative compounds

103 Compound ST1

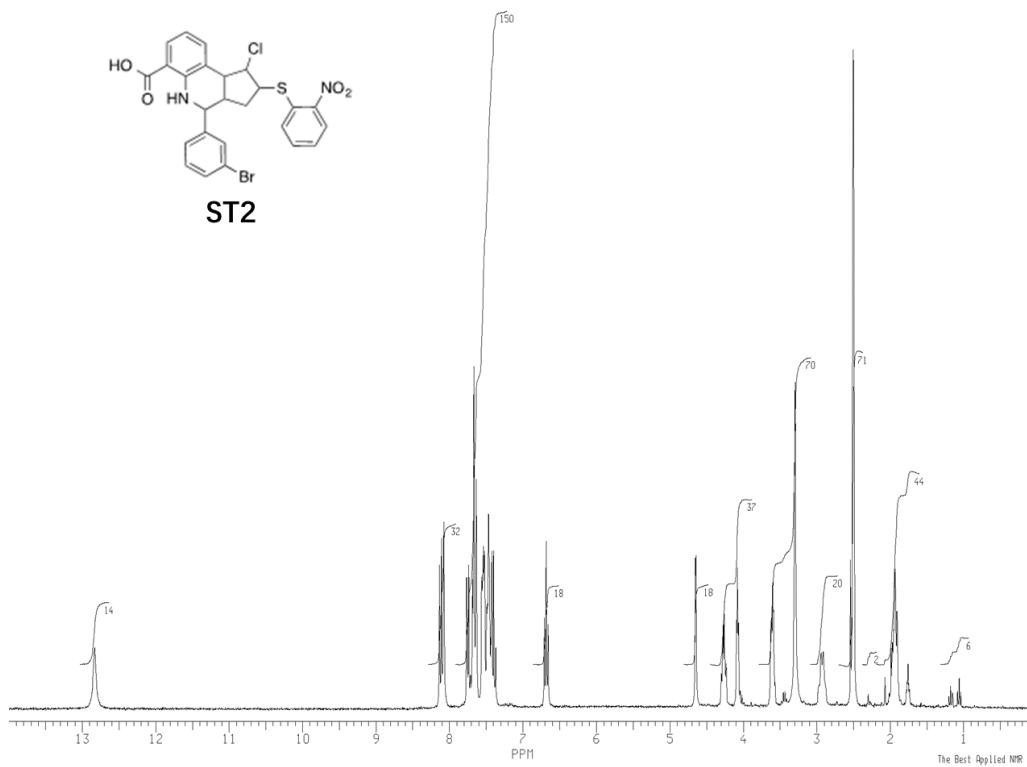


104

105

106 Compound ST2

© N.D. Zelinsky Institute of Organic Chemistry (Moscow), Bruker AM300 SF=300.13 MHz[H-1] SI=16K SR=6024 01=7180 PM=4 AQ=1.3599 RD=3 NS=16 SR=4787.839 TE: A6-205/13052034

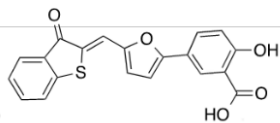


107

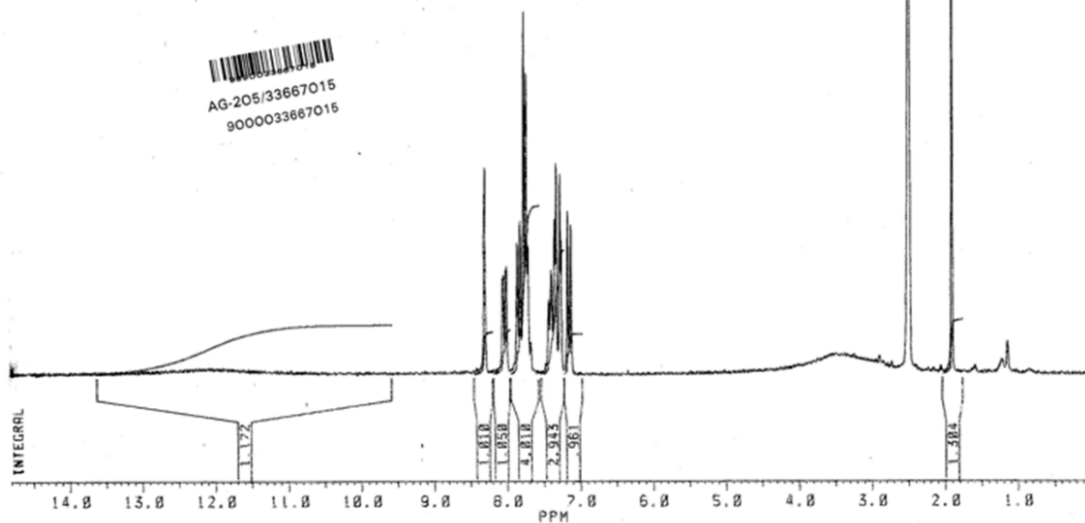
108

109

110 **Compound ST3**



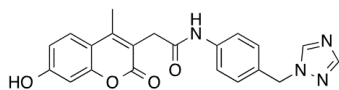
ST3



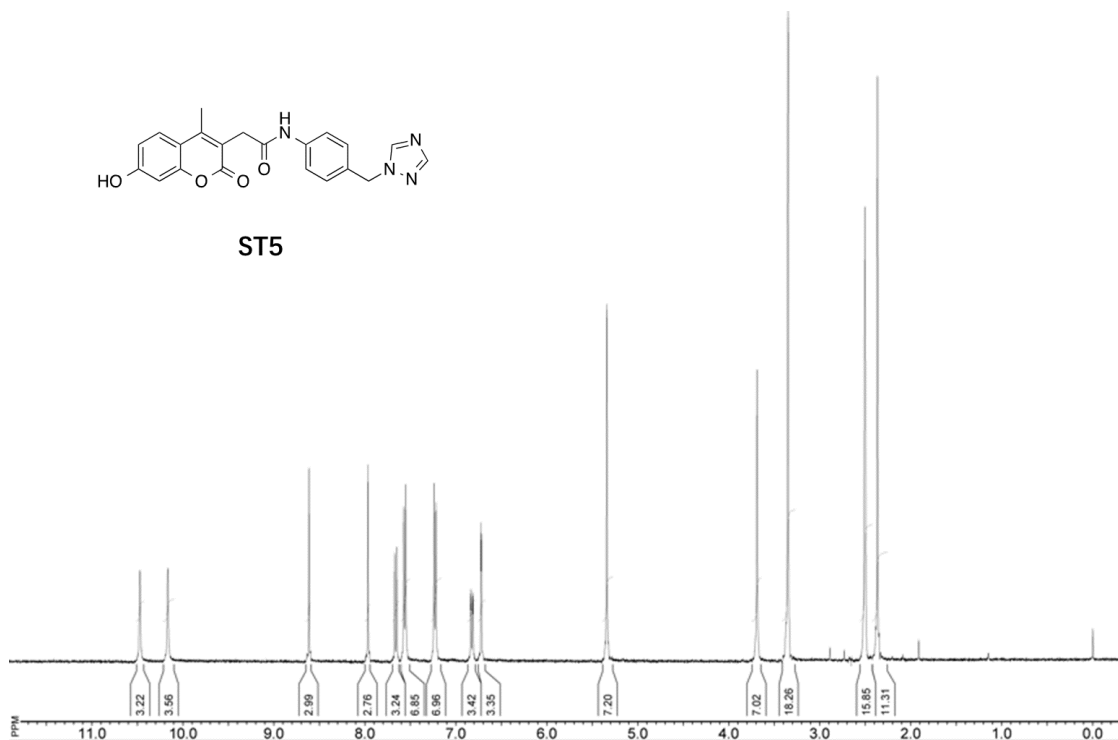
111

112

113 **Compound ST5**



ST5

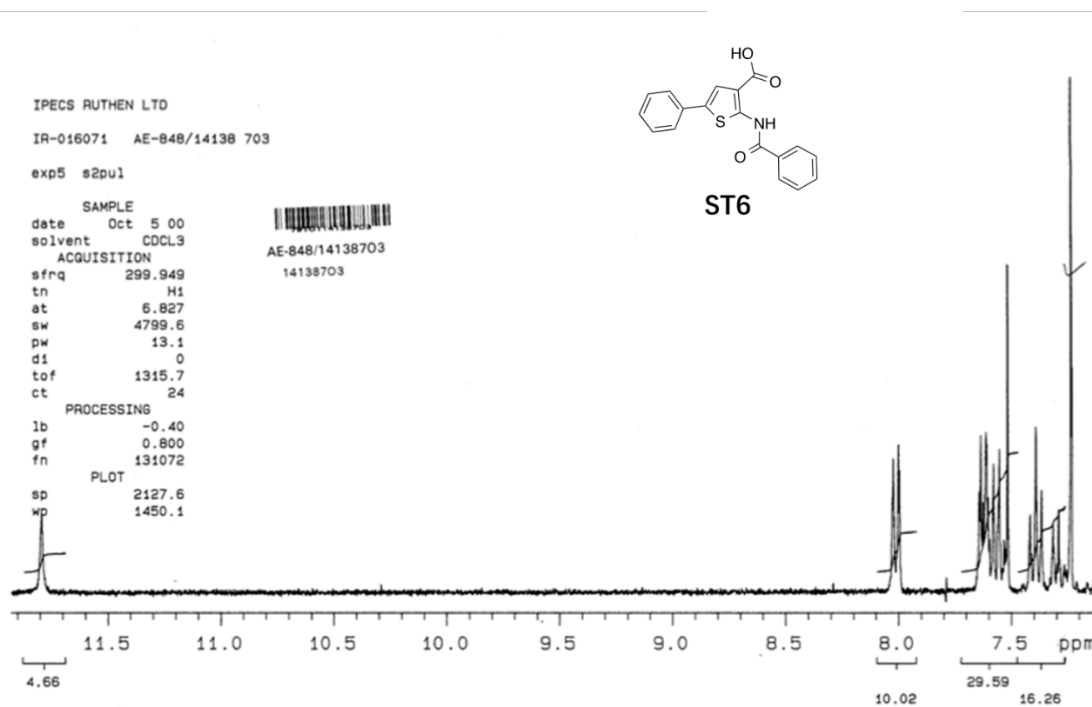


114

115

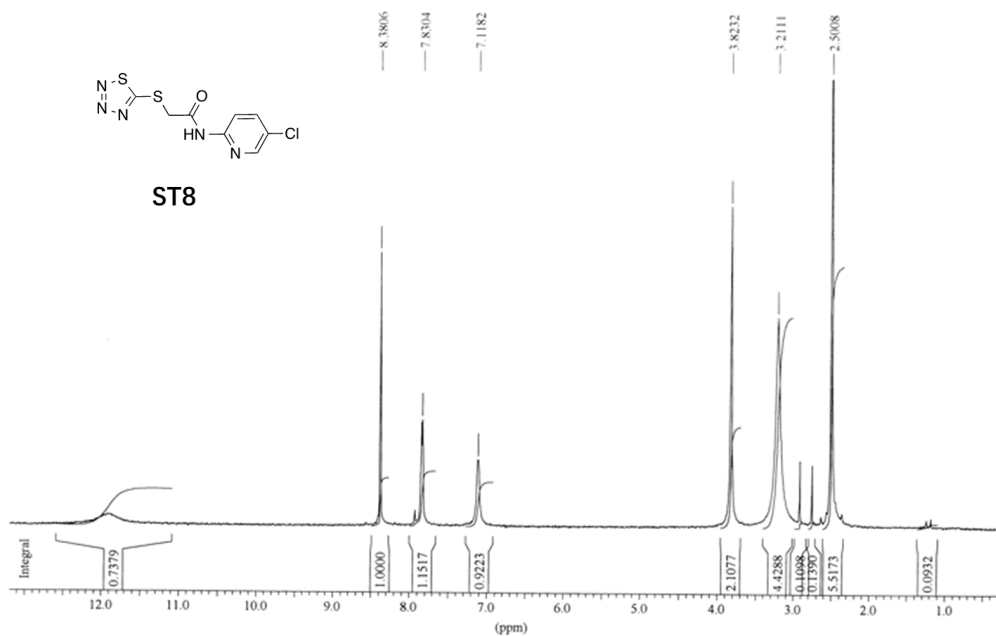
116

117 **Compound ST6**



118

119 **Compound ST8**



120

121

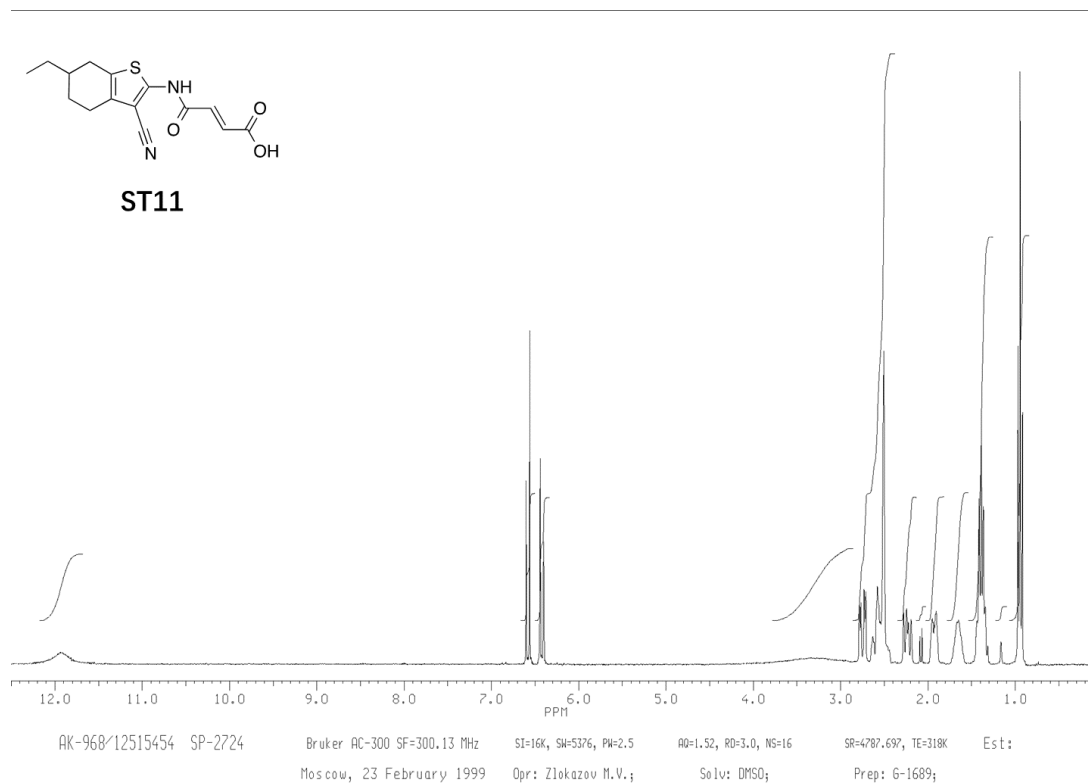
122

123

124

132

133 **Compound ST11**



134